

INTERIM REPORT 1

Improving earthquake monitoring for gravitational-waves detectors with historical seismic data

SKY SOLTERO

ABSTRACT

A remarkable level of isolation from the ground is required for Advanced gravitational-wave detectors such as the Laser Interferometer Gravitational-Wave Observatory (LIGO) to function at peak performance. These ground based detectors are susceptible to high magnitude teleseismic events such as earthquakes, which can disrupt proper functioning, operation and significantly reduce their duty cycle. As a result, data is lost and it can take several hours for a detector to stabilize and return to the proper state for scientific observations. With advanced warning of impending tremors, the impact can be suppressed in the isolation system and the down time can be reduced at the expense of increased instrumental noise. An earthquake early- warning system has been developed relying on near real-time earthquake alerts provided by the U.S. Geological Survey (USGS) and the National Oceanic and Atmospheric Administration (NOAA). The alerts can be used to estimate arrival times and ground velocities at the gravitational-wave detectors. By using machine learning algorithms, a prediction model and control strategy has been developed to reduce LIGO downtime by 30%. This paper presents further improvements under consideration to better develop that prediction model and decrease interruptions during LIGO operation.

INTRODUCTION

The two detectors that compose the Laser Interferometer Gravitational-Wave Observatory (LIGO) along with Virgo, and GEO600 detectors form a global network of gravitational wave interferometers. Keeping the detectors in operating mode requires an exceptional level of isolation from the ground so that the cavities can be held in optical resonance and be capable of observing displacements in space-time of less than one thousandth of the diameter of a proton. Environmental disturbances such as earthquakes can disrupt operating mode, destabilize detectors and cause the detectors to fall out of lock despite seismic isolation systems already in place to minimize interfering effects. When the detectors have fallen out of lock, where the control system cannot maintain optics at their stabilized positions, it can take many hours to return to the locked state and normal operation. During the observation run (referred as O1), from January 18, 2015 to January 12, 2016 operation was disrupted 62 times at LIGO Hanford and 83 times at LIGO Livingston due to earthquakes. Previous studies have shown that by using an early-warning earthquake system, relying on alerts provided by the U.S. Geological Survey (USGS) and the National Oceanic and Atmospheric Administration (NOAA), arrival times and ground velocities could be predicted which have a direct correlation with the operation status of the interferometers (Coughlin et al. 2017). The higher the incoming

seismic velocities the more unstable the interferometer. A strategy intended to maintain lock and suppress these seismic disturbances early in the isolation system, at the expense of sensitivity and increased noise, would notably increase the interferometers' duty cycle (Biscans et al. 2018). Consequently, an earthquake early warning application named Seismon has been created to process real-time alerts from the USGS containing specific characteristic information about the earthquakes to provide estimated arrival times of the seismic phases and seismic amplitudes of the surface waves at the detector sites. By implementing detector control configurations, it is predicted that 40 to 100 earthquake operation interruptions could be prevented in a 6-month period.

OBJECTIVES

We aim to improve the algorithms of Seismon and as a result reduce LIGO downtime and increase the time the detectors are in observing mode. The alerts received from USGS contain information on time, location, depth, and magnitude of a specific earthquake which is then used to predict ground velocities, arrival time and amplitude of the various seismic phases at the detector sites. Seismon initially relies on earthquake notifications from a worldwide network of seismometers. P-waves (primary) traveling twice as fast as S-waves (secondary) reach the seismic stations first, thus providing the initial earthquake character estimations. As more and more data is acquired solutions to

the hypocenter and magnitude of the earthquake are estimated and the solutions are sent to USGS's Product Distribution Layer (PDL). This ensures Seismon receives the most pertinent notifications. From there the notifications are processed to predict the seismic wave arrival time and the amplitude of the ground motion at the detectors. Past earthquake records and the seismic data at the detectors are also examined to predict how the ground motion will affect the observatories. The predicted amplitude and past earthquake data are compared, with the difference being minimized by adaptive simulated annealing algorithms to obtain solutions close to the global minima. Lastly, the predictions are used to create warnings delivered to the detectors containing the amplitude prediction, lockloss probability and the anticipated earthquake arrival time at the observatories. Seismon performance can be evaluated by recording and analyzing the notification duration, accuracy of predicted ground-motion amplitude, time-of-arrival predictions and the detector lockloss predictions. Current evaluations with the LIGO Observing Run 1 from September 2015 to January 2016, show about 90% of seismic events are within a factor of 5 of the predicted ground velocity and within 3s of the final predicted arrival time (Coughlin et al. 2017). Examining the times lockloss occurred, it can be said that the detectors generally fall out of lock at ground velocities greater than $5 \mu\text{m/s}$ but at lower velocities the data is more complex. Therefore, incorporating more ways of determining better lockloss predictions are of interest and would demonstrate success in this project. We purpose to improve the Seismon algorithm by incorporating more machine learning methods, broadening ground motion parameters and collecting more accurate data to enrich the prediction models.

APPROACH

We intend on advancing the Seismon application by improving predictions and acquiring more data of various parameters of incoming teleseismic events. We will test if the arrival time predictions can be improved by machine learning algorithms. To enhance ground velocity predictions, we will explore broadening our data resources and determine if we can acquire more data from hundreds of other seismic stations around the United States and the world. In addition, we would like to discover if we can use moment tensor data to further improve velocity predictions.

PROJECT SCHEDULE

I propose the following analysis and timeline for improving the code base: **1.** (week 1-3) Understanding

how magnitude and location play a role in different velocity estimations. Running and understanding existing machine learning infrastructure. **2.** (week 4-6) Applying existing methods to broader seismic datasets. Creating a world grid with approximate earthquake velocities at various sections of the earth's surface based on historic data. **3.** (week 7-10) Employing machine learning algorithms to improve on the existing algorithms.

1. RESULTS (IN PROGRESS)

To better understand the effects of earthquake magnitude and global location on arriving earthquake surface velocities at the detectors, multiple plots using historical data have been made. In Figure 1, earthquake velocities are determined by dividing the distance from earthquake origin to detector by the difference of P-surface wave prediction times and earthquake times. These earthquake velocity magnitudes are then plotted at their origin in regards to latitude and longitude.

These plots show velocities reaching up to 16,000 m/s, which is higher than expected for simple P-waves. To explore the contributions of reflections internal to the Earth, in Figure 2, the effective velocities of the paths that include reflections (left) and those that do not (right). These velocities are shown on a grid of depth and degrees. While the plot on the right is in line with expectations for P-wave velocities, the plot on the left shows the contributions from reflections, leading to much higher effective velocities (and therefore faster arrivals). This result shows that the first arrivals of the P-waves shown in Figure 1 derive from P-waves reflecting in the Earth.

We now explore the velocities in real data measured from seismometers at the Hanford and Livingston sites. Figure 3 show the effective earthquake velocity, measured as the distance of the earthquake divided by the difference of the peak ground velocity time and earthquake time. It shows a range of velocities from 2000 to 5000 m/s which is appropriate for surface wave velocities dominating the time-series, as expected. We include only the historical data with peak ground velocities greater than $1 \mu\text{s}$.

To understand the frequency of earthquakes at certain velocities, Figure 4 shows a histogram corresponding to the data used for Figure 3. These plots show that the majority of earthquakes have effective velocities between 2000 and 4000 m/s, as expected for surface waves. The outliers are likely either body wave contributions or contamination from other earthquakes.

With a large amount of historical data, featuring earthquakes of magnitude 6 or higher a world map taking the averages of multiple known earthquake veloci-

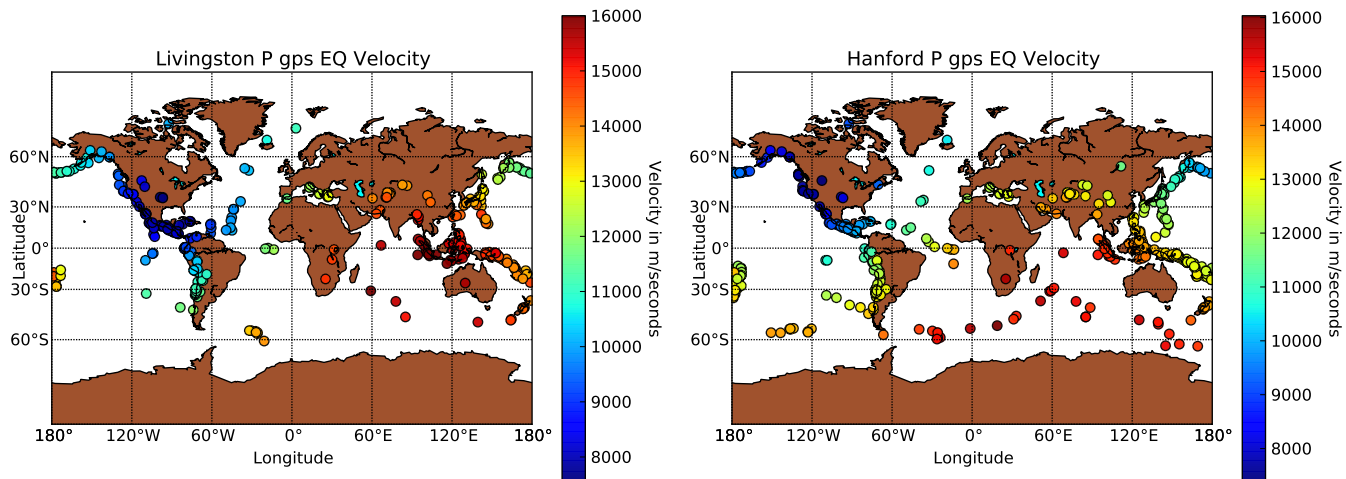


Figure 1. Magnitude of earthquake (EQ) velocities based on data using P-wave arrival times plotted at corresponding latitude and longitude points. Data with peak ground velocities less than $1 \mu/s$ have been omitted. Displayed on the left is the plot for Livingston data and on the right is the plot for Hanford data.

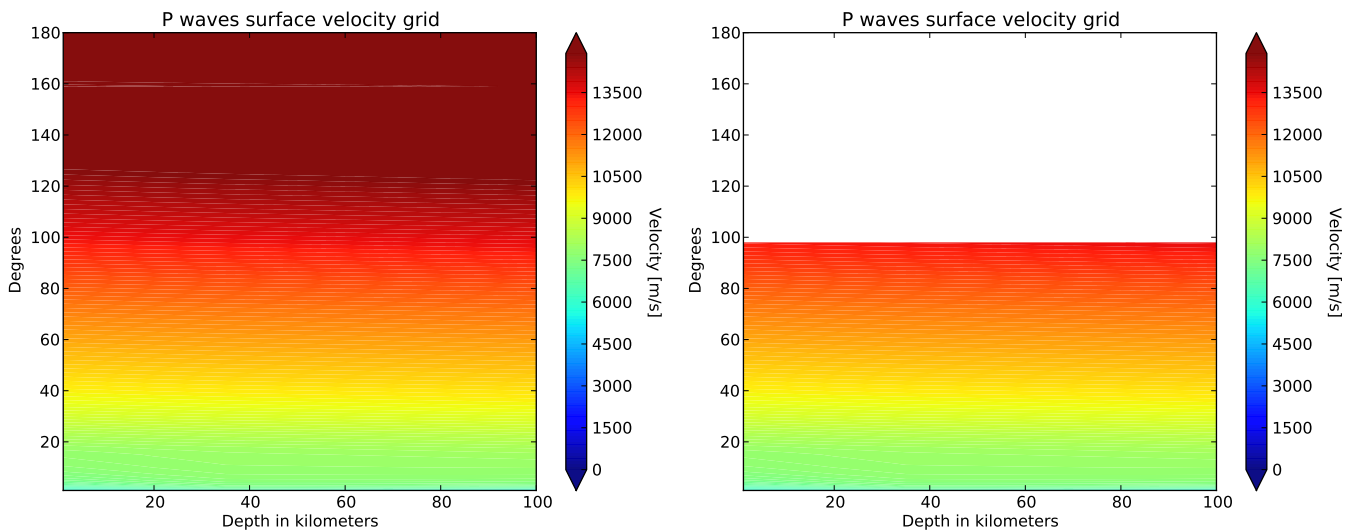


Figure 2. Magnitude of Earthquake velocities based on data using P-wave arrival times plotted in accord to degrees and dept of earthquake origin. Displayed on the left plot is the velocity without taking into account reflections. On the right plot reflections are taken into account and more expected P-wave velocities are shown.

ties crossing a portion of the grid was plotted. This was completed with the hope of being able to show how the earthquake velocity changes depending on what portion of the earth it's traveling through. Since the earthquake data ranged widely in velocity values due to other factors, the map as a whole became too averaged overall and did not provide any useful information. A smaller map of the United States with the same purpose except taking in only western hemisphere earthquakes was also plotted in Figure 5. It's assumed the velocities are still being over averaged and further exploration to provide more accurate data input as a way of producing a more beneficial map are to be explored. Different experimentation in machine learning also led to some favorable results. Using a neural network, hundreds of thousands of historic earthquakes surrounding regions local to the United States, greater than magnitude 6 and occurring only on land were used to train a model based on known ground velocities. A random omitted portion of that data was then tested upon to predict ground velocities with a majority of the predictions falling under a factor of two of the actual value. This factor of two is determined by taking the difference of the predicted and actual ground velocities and then dividing by the actual. A histogram displaying the amount of data falling within these factors is displayed in figure 7. In figure 6, the neural network predicted ground velocities versus the actual ground velocities were plotted against each other for comparison. We expect to see the predicted and actual ground velocities plotted following a slope of 1. The more fitting to the slope line shown, the more accurate the predictions. For this particular plot the loss in training was .2201. A graph showing the density of where these points fall along the slope line is also shown.

To check the type of earthquake data being fed into the model is accurate and useful in itself, a plot of distance versus time was produced. The three labeled lines show where known rayleigh waves at different velocities would be represented in this graph. A corresponding graph showing the particular density of where these points fall along the slope line is also shown. Now that it is known we can predict ground velocities under a factor of two successfully further exploration in improving the neural network, filtering more accurate training data, and using the neural network to predict arrival times themselves will be made.

INTERIM REPORT 2

WORK DONE

Some of the work I have done over the pass month include making more accurate plots displaying earthquake surface velocities, experimenting with machine

learning scripts, and sorting data. I have experimented with a collaborator's machine learning script and attempted to reproduce results that show satisfactory predictions in earthquake ground velocities. The results weren't as definite as expected so I tried testing the model against the same data it was trained on and the results did not improve. At the same time I made a world grid that took in thousands of earthquakes velocities detected at multiple seismometers and averaged out the earthquake velocity for each grid space. I experimented with changing parameters in the data such as where the earthquake occurred, ground velocity speeds, seismometer locations and if the earthquake and seismometer were located on land or not. After the first machine learning script I then experimented with a neural network learning script that produced much more promising results. With this data I have made various plots to show how the ground velocity predictions compare to the actual ground velocity values.

PROGRESS

Some of the progress I have made so far have been in the experimentation of machine learning scripts and producing plots that display global and local earthquake velocities more accurately . With one machine learning script based on scores, I was not able to produce satisfactory results so these observations are not what we were expecting. However with a neural network I was able to observe more desired results. With the neural network script taking in earthquake data only from the western hemisphere and occurring on land I was able to predict ground velocities with the majorities of predictions falling within a factor of two of the actual ground velocities. The next step would be to further see if we can improve the model by adding more layers and being more specific with the training data inputted. Also I have made progress in making grids of the world and the United states that take in hundreds of thousands of earthquake velocities and then averages the velocity for that portion of the grid. By changing the parameters of the earthquakes and the seismometers included in the data the plot results differ vastly. Therefore I was also able to continue to experiment with different historical data and try to produce a grid that more accurately displays velocities at different points in the grid.

CHALLENGES

Some of the challenges I have met so far are conceptually understanding the data for different seismic phases

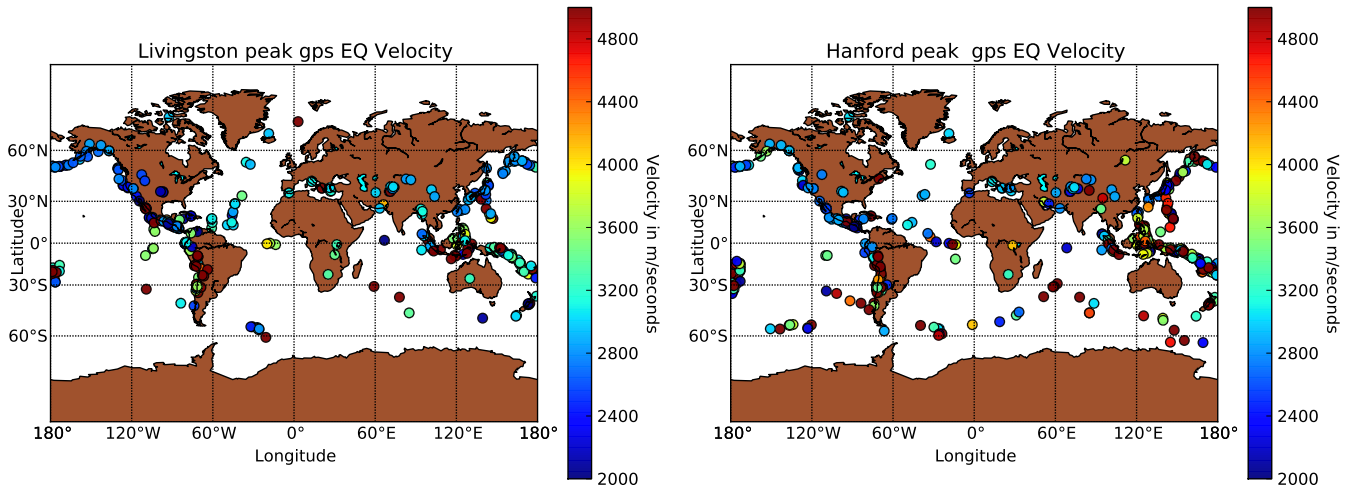


Figure 3. Magnitude of earthquake (EQ) velocities based on data using peak ground velocity gps time plotted at corresponding latitude and longitude points. Data with peak ground velocities under $1e-6$ have been omitted. Displayed on the left is the plot for Livingston data and on the right is the plot for Hanford data.

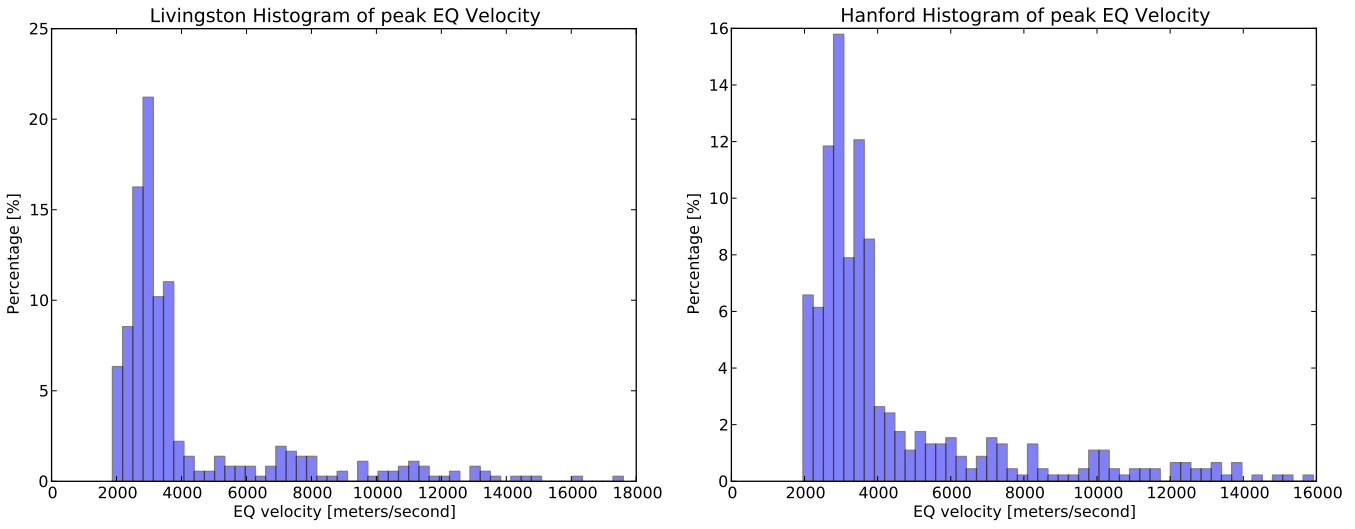


Figure 4. Percentage of different earthquake (EQ) velocities based on data using peak ground velocity gps time divided by the distance from the detectors. In association with the above Figure 2 plots. Data with peak ground velocities less than $1 \mu/s$ have been omitted. Displayed on the left is the plot for Livingston data and on the right is the plot for Hanford data.

and how they affect the earthquake velocity that we are concerned about and the detectors. Additionally, understanding the neural network script and the improvements that could be added to the network is also a subject to study further. Some of the challenges I anticipate are creating more complex graphs due to the processing of data inputted.

GOALS

My research goals for the rest of the summer is to continue to improve the neural network model and ap-

ply the model to arrival times successfully. I would also like to understand how to incorporate and filter more earthquake data for the training model so that it may be trained as accurately as possibly. Lastly, I would still like to experiment with producing more accurate world and United States grids that display averaged earthquake velocities for a specific portion of that grid. These goals have changed slightly. I still want to predict arrival times as accurately as possible but I've learned having a greater understanding of type of earthquake data and how to filter it may be of importance to bettering the neural network model.

REFERENCES

Biscans, S., Warner, J., Mittleman, R., et al. 2018, Classical and Quantum Gravity

Coughlin, M., Earle, P., Harms, J., et al. 2017, Classical and Quantum Gravity, 34, 044004

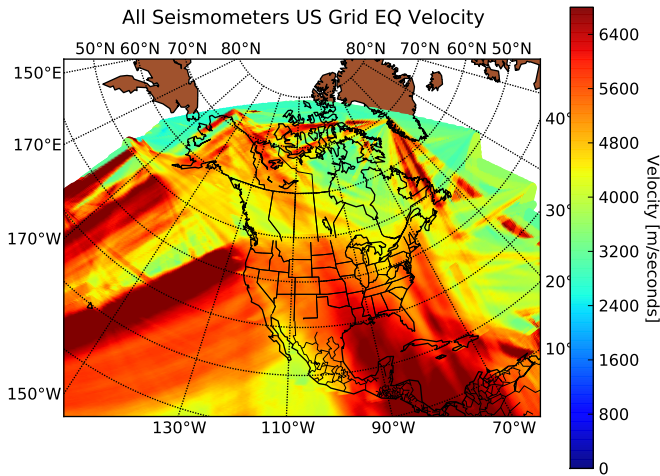


Figure 5. United states grid representing various averaged earthquake velocities over numerous grid portions. The earthquake velocity data representing this grid were taken from earthquakes higher than magnitude 6, only within the areas on and surrounding the United States and those earthquakes which occurred on land.

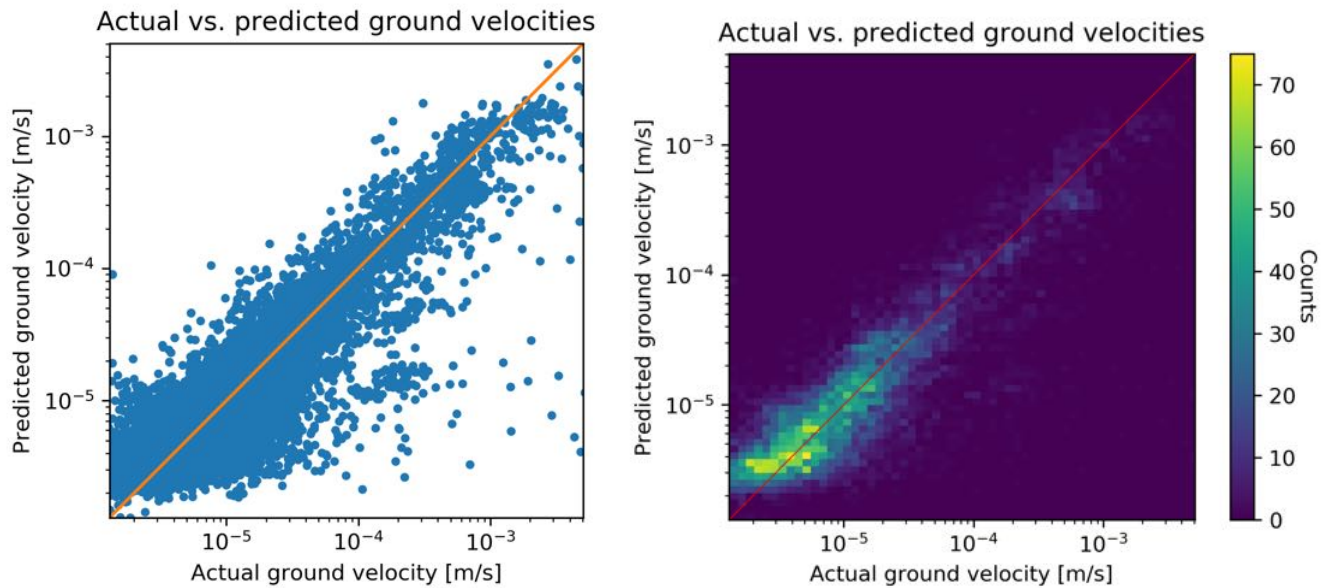


Figure 6. Ground velocity predictions versus Actual ground velocities is displayed on the left plot. The closer the points displayed are to the trend line of 1, the more accurate the prediction. A density plot of the same graph for easier visualization of data is shown on the right.

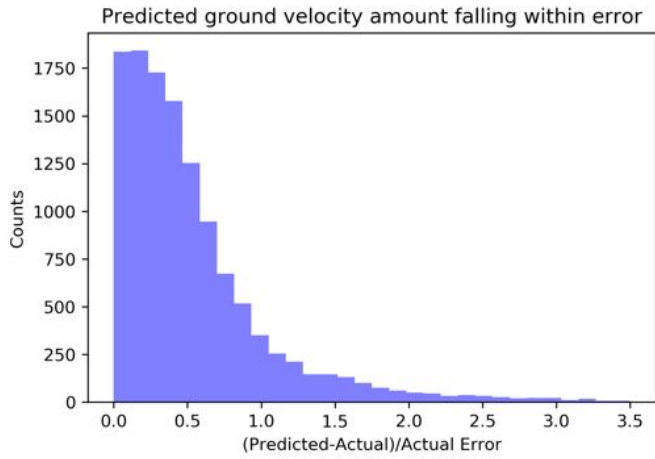


Figure 7. A histogram displaying the counts of ground velocity predictions within a factor of error representing the same data corresponding to figure 7.

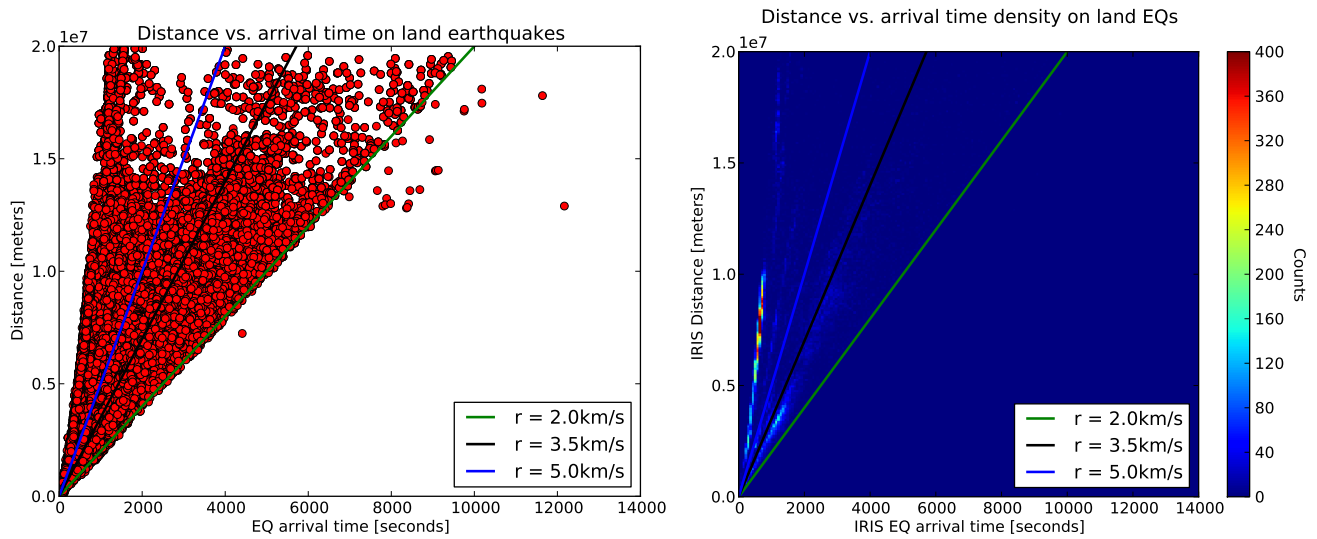


Figure 8. The distance versus arrival times of the input data used to train the neural network model and produce Figure 6 graphs. The solid slope lines represent different rayleigh wave speeds commonly observed. A density plot of the same graph for easier visualization of data is shown on the right.